

TECHNICAL NOTE

Evaluation of Thin-slice Coronal Single-shot Turbo Spin-echo Diffusion-weighted Imaging of the Hand: A Comparison with Conventional Echo-planar Diffusion-weighted Imaging

Masaki Ogawa^{1*}, Motoo Nakagawa¹, Nobuyuki Arai², Hirohito Kan²,
Shota Ohba¹, Shunsuke Shibata¹, Hiroyuki Maki¹, and Yuta Shibamoto¹

We prospectively evaluated thin-slice coronal turbo spin-echo (TSE) diffusion-weighted imaging (DWI) covering a larger area with the recently-developed techniques on a 3T MRI scanner, compared with echo-planar imaging (EPI)-DWI in patients undergoing routine hand MRI. Visual score assessment and apparent diffusion coefficient (ADC) measurement were performed for patients with suspected hand tumors. TSE-DWI was superior to EPI-DWI, with less image distortion. The visual score and ADC comparison assessments proved that the image noise of TSE-DWI was acceptable.

Keywords: *musculoskeletal lesion, magnetic resonance imaging, non-echo-planar imaging technique, turbo spin-echo diffusion-weighted imaging*

Introduction

Diffusion-weighted imaging (DWI), a non-contrast imaging technique, is widely used to evaluate both intracranial and extracranial tumors.¹ Many studies have reported that apparent diffusion coefficient (ADC) values are useful in distinguishing between malignant and benign musculoskeletal tumors.² A coronal DWI scan can cover a larger area of the hand than axial DWI and might be useful for evaluating multiple lesions, arthritis, or tendinitis. For example, assessment of rheumatoid arthritis using DWI was reported previously.³ However, on coronal DWI with echo-planar imaging (EPI), especially when evaluating a hand or foot, severe image distortions due to susceptibility artifacts and chemical shift artifacts degrade lesion conspicuity.^{1,4} Single-shot turbo spin-echo (TSE) DWI reduces these image distortion and chemical shift artifacts, but severe image noise and blurring degrade the image quality and ADC measurements.⁴ Recently, parallel imaging technique and higher signal-to-noise ratio (SNR) at 3T improved these issues with single-shot TSE-DWI.^{1,4} The utility of TSE-DWI has been reported in evaluations of middle ear cholesteatoma, orbital and neck lesions,

breast and lung cancers, and spinal cord infarction.^{1,5–10} To the best of our knowledge, however, there have been no TSE-DWI studies evaluating musculoskeletal lesions of the hand or foot. In addition, only one previous case report evaluated middle ear cholesteatoma using 2-mm-thick single-shot TSE-DWI, but ADC measurement was not performed and the acquisition time was not presented.⁶

TSE-DWI using the recently-developed parallel imaging and single-shot technique on 3T MRI might yield a superior image quality and is already used clinically. However, the image quality of thin-slice TSE-DWI for the assessment of small musculoskeletal lesions has not yet been clarified. Thus, the purpose of this study was to prospectively examine whether the 2-mm-thick coronal TSE-DWI covering a larger area and small lesions could substitute for conventional EPI-DWI in patients undergoing routine hand MRI on a 3T scanner.

Materials and Methods

Study design

This prospective study was performed in accordance with the ethical standards of our Institutional Review Board. Written informed consent was obtained from the patients and their privacy was completely protected. Eligibility criteria for entry were: (1) adult patients suspected of having or being followed for a musculoskeletal tumor of the hand or finger, (2) patient agreement to cooperate, and (3) examination on a Philips 3T MRI scanner (Ingenia; Philips Medical Systems, Eindhoven, The Netherlands). The exclusion criteria were: (1) contraindications to MR (incompatible metal implants or pacemakers), and (2) motion artifacts and artifacts from unsuppressed fat on the images. The primary

¹Department of Radiology, Nagoya City University Graduate School of Medical Sciences, Aichi, Japan.

²Department of Radiology, Nagoya City University Hospital, Aichi, Japan.

*Corresponding Author: Department of Radiology, Nagoya City University Hospital, 1 Kawasumi, Mizuho-cho, Mizuho-ku, Nagoya, Aichi 467-8601, Japan. Phone: +81-52-853-8276, Fax: +81-52-852-5244, E-mail: eternal@fj9.so-net.ne.jp

©2019 Japanese Society for Magnetic Resonance in Medicine

This work is licensed under a Creative Commons Attribution-NonCommercial-NoDerivatives International License.

Received: June 20, 2019 | Accepted: September 18, 2019

endpoint of the study was assessment of the image quality and artifacts with 4-point scales. The secondary endpoint was comparison of ADC, as described in detail below. To detect a difference of 1 in scores of visual evaluations for paired samples, 13 patients were considered necessary with a power of 0.9 and two-sided P of 0.05 if the standard deviation (SD) was assumed to be 1.0. If the SD was 1.5, 26 patients were considered necessary. In previous studies using point scales,^{5,8} the SDs for the visual scores were no more than 1.0, and so we hypothesized that the SD might not exceed 1.5. Therefore, we aimed to enroll 26 patients in this study.

Between June 2017 and February 2018, a total of 26 patients (23–79 years with a median age of 52 years; nine men and 17 women) entered the study and underwent MRI with EPI-DWI and TSE-DWI sequence on the their clinical diagnoses were ganglion ($n = 4$), enchondroma ($n = 4$), neurogenic tumor ($n = 3$), fibroma ($n = 3$), giant cell tumor of tendon sheath ($n = 2$), glomus tumor ($n = 1$), atheroma ($n = 1$), postoperative change ($n = 6$), and no lesion ($n = 2$).

MRI technique

All MRI images were obtained on a 3T MRI scanner (Ingenia; Philips Medical Systems, Eindhoven, The Netherlands) using an eight-channel SENSE hand-wrist surface coil. Coronal 2-mm-thick TSE-DWI and EPI-DWI were performed after routinely obtaining two-dimensional T_1 -, T_2 -weighted images, and fat-saturated T_2 -weighted images. The fat saturation technique using spectral attenuated inversion recovery technique was applied for TSE-DWI and EPI-DWI. Each DWI sequence was scanned with the parameters shown in Table 1. ADC maps for both TSE-DWI and EPI-DWI were calculated by using the software of the scanner.

Table 1 Imaging parameters for TSE-DWI and EPI-DWI

	TSE-DWI	EPI-DWI
TR (ms)	7000	2500
TE (ms)	68	64
Flip angle (°)	90	90
Echo train length	23	23
b -values (s/mm ²)	0, 800	0, 800
Bandwidth (Hz/pixel)	665	1777
FOV (mm)	150	150
Matrix	80 × 64	80 × 64
Matrix size/slice thickness (mm)	1.9/2.0 (slice gap: 0.2)	1.9/2.0 (slice gap: 0.2)
Number of signals averaged	4	8
Sensitivity encoding factor	2	2
Scan time	196	143

TSE-DWI, turbo-spin echo DWI; EPI-DWI, echo-planar imaging-diffusion-weighted imaging.

Image data analysis

For visual evaluation and ADC measurement of the lesions, all images were presented in random order using PACS software (EV Insite R, PSP Corporation, Tokyo, Japan) and 3-megapixel monitors (Totoku, Tokyo, Japan) that allowed adjustment of the window and level settings. Readers were blinded to the clinical information.

The visual evaluations were independently carried out by two radiologists (M.N. and S.O.: readers 1 and 2). TSE-DWI and EPI-DWI ($b = 800$ s/mm²) images, both with ADC maps, were evaluated in separate viewing sessions at intervals of at least two weeks following previous visual evaluation studies,¹¹ referring to T_2 -weighted or other images. The degree of lesion conspicuity, image distortion, image noise, and overall image quality were visually graded with 4-point scales: score 1, unacceptable; score 2, poor; score 3, moderate; score 4, good. For the degree of lesion conspicuity, the score was judged as 2 when the lesion was visualized on DWI images and measurement of ADC values were affected by artifacts.

Apparent diffusion coefficient measurements of the lesions were independently carried out by two other radiologists (M.O and S.S.: readers 3 and 4). The lesions were visually identified on TSE-DWI and EPI-DWI images with ADC maps in the same viewing sessions. ADC measurements were not performed when lesions were not detected, showed low intensity on each DWI image, or were affected by artifacts on ADC maps. Each reader manually placed two or three small elliptical regions of interest (ROIs) on the lowest values on the ADC map within visually artifact-free and homogeneous low-value areas in the lesions and with enough distance from the edge. For each ADC map of TSE-DWI and EPI-DWI, similar ROIs were placed using copy and paste. The lowest mean ADC value of the small ROIs was used for the minimum ADC value, in accordance with previous studies.^{2,12} For the measurements of ADC values of a whole lesion, as large ROIs as possible were placed on the ADC map within visually artifact-free areas in the lesion with enough distance from the edge for each ADC map and the mean ADC value was used.

Signal-to-noise ratio calculations were carried out using the identical ROI method described previously.¹¹ The ROIs were manually selected within homogeneous and artifact-free areas in the muscle on DWI images. Similar ROIs were placed using the copy-and-paste method for each TSE-DWI and EPI-DWI. The mean signal intensity (SI) and SD were measured in the ROIs, and the SNR was calculated as follows:

$$\text{SNR} = \frac{\text{SI}}{\text{SD}}$$

Statistical analysis

Statistical analysis was performed using BellCurve for Excel version 2.11 (Social Survey Research Information Co., Ltd., Tokyo, Japan). We used the Wilcoxon signed-rank test for non-normally distributed data. $P < 0.05$ was considered indicative of a significant difference. Interobserver agreement and

agreement between ADC measurements of TSE-DWI and EPI-DWI were evaluated by using an inter-class correlation coefficient (ICC 2, 1), according to a previous study.¹⁰ We recorded the strength of agreement as poor (ICC = 0.00–0.20), slight (ICC = 0.21–0.40), fair (ICC = 0.41–0.60), moderate (ICC = 0.61–0.80), or excellent or perfect (κ = 0.81–1.00).

Results

The results of visual score assessment for TSE-DWI and EPI-DWI and inter-observer agreement for the two readers are presented in Table 2. Moderate to perfect inter-observer agreements were obtained between the two readers

(ICC = 0.61–1.00). The lesion conspicuity score, image distortion score, and overall image quality score were rated significantly higher for TSE-DWI [mean (\pm SD) scores of the two readers: 3.8 ± 0.4 , 4.0 ± 0.2 , and 3.7 ± 0.5 , respectively] than for EPI-DWI (2.3 ± 0.7 , 2.3 ± 0.7 , and 2.4 ± 0.8 , respectively: $P < 0.01$). The image noise score for TSE-DWI (mean score of the two readers: 3.2 ± 0.5) was slightly lower than that for EPI-DWI (3.4 ± 0.6), but there was no significant difference ($P = 0.18/0.09$ for each reader).

For ADC measurement of the lesions, both readers excluded the same 11 cases, and ADC measurements were carried out for the other 15 lesions (4–35 cm with a median size of 11 cm), summarized in Table 3. The minimum ADC

Table 2 Mean scores for visual assessment of TSE-DWI and EPI-DWI and inter-observer agreement for two readers

	Reader 1			Reader 2			ICC for two readers	
	TSE-DWI	EPI-DWI	P-value	TSE-DWI	EPI-DWI	P-value	TSE-DWI	EPI-DWI
Lesion conspicuity	3.8 ± 0.4	2.3 ± 0.7	<0.01	3.9 ± 0.4	2.4 ± 0.8	<0.01	0.76	0.90
Image distortion	4.0 ± 0.2	2.3 ± 0.7	<0.01	4.0 ± 0.2	2.4 ± 0.8	<0.01	1.00	0.81
Image noise	3.2 ± 0.5	3.4 ± 0.6	0.18	3.3 ± 0.5	3.6 ± 0.6	0.09	0.71	0.61
Over all image quality	3.7 ± 0.5	2.4 ± 0.8	<0.01	3.8 ± 0.4	2.5 ± 0.8	<0.01	0.70	0.87

Values are mean \pm standard deviation. TSE-DWI, turbo-spin echo DWI; EPI-DWI, echo-planar imaging DWI; ICC, inter-class correlation coefficient.

Table 3 Minimum and average ADC values ($\times 10^{-3}$ mm²/s) of 15 lesions in TSE-DWI and EPI-DWI for two readers

Case no	Reader 1				Reader 2			
	Minimum		Average		Minimum		Average	
	TSE-DWI	EPI-DWI	TSE-DWI	EPI-DWI	TSE-DWI	EPI-DWI	TSE-DWI	EPI-DWI
1	1.20	1.15	1.44	1.30	1.28	1.12	1.50	1.40
2	1.90	2.06	1.88	2.04	1.83	1.87	1.88	2.01
3	1.37	1.41	1.57	1.65	1.39	1.42	1.59	1.58
4	3.01	2.97	2.96	2.99	3.01	2.92	2.97	3.05
5	0.66	0.77	0.65	0.81	0.73	0.82	0.65	0.94
6	1.36	1.30	1.49	1.51	1.35	1.25	1.48	1.48
7	1.53	1.64	1.87	1.64	1.61	1.64	1.84	1.63
8	2.56	2.27	2.57	2.34	2.56	2.34	2.56	2.36
9	1.34	1.38	1.58	1.40	1.31	1.26	1.57	1.43
10	1.50	1.32	1.57	1.40	1.31	1.25	1.54	1.32
11	1.75	1.65	1.78	1.65	1.72	1.67	1.72	1.66
12	1.35	1.49	1.41	1.52	1.21	1.20	1.36	1.33
13	2.39	2.46	2.43	2.40	2.47	2.44	2.42	2.41
14	1.99	1.91	1.94	1.97	1.99	1.91	1.98	1.94
15	2.81	2.70	2.81	2.88	2.43	2.46	2.72	2.61
ICC for TSE-DWI and EPI-DWI	0.98		0.97		0.99		0.97	
ICC for two readers	0.98	0.98	1.00	0.99				

TSE-DWI, turbo-spin echo DWI; EPI-DWI, echo-planar imaging DWI; ICC, inter-class correlation coefficient.

values in TSE-DWI and EPI-DWI showed excellent agreement (ICC = 0.98 and 0.99, respectively, for the two readers): 1.78 ± 0.66 and $1.77 \pm 0.62 \times 10^{-3} \text{ mm}^2/\text{s}$, respectively, for reader 3; 1.75 ± 0.63 and $1.70 \pm 0.61 \times 10^{-3} \text{ mm}^2/\text{s}$, respectively, for reader 4. The average ADC values in TSE-DWI and EPI-DWI also showed excellent agreement (ICC = 0.97 for both readers): 1.86 ± 0.61 and $1.83 \pm 0.60 \times 10^{-3} \text{ mm}^2/\text{s}$, respectively, for reader 3; 1.85 ± 0.60 and $1.81 \pm 0.58 \times 10^{-3} \text{ mm}^2/\text{s}$, respectively, for reader 4. Excellent inter-observer agreement was obtained between the two readers (ICC = 0.98–1.00). The SNR values in TSE-DWI and EPI-DWI were 14.9 ± 6.6 and 19.2 ± 5.5 , respectively. TSE-DWI showed significantly lower SNR than EPI-DWI ($P < 0.01$).

Representative cases are presented in Figs. 1–3. On TSE-DWI images and the ADC maps, the lesions of these three cases were clearly visualized with acceptable image noise. On EPI-DWI images, the lesion in Fig. 1 was shown but affected by distortion artifacts; the lesion in Fig. 2 was depicted but the ADC value could not be measured due to artifacts; and the lesion in Fig. 3 could not be visualized on the EPI-DWI image or ADC map due to strong distortion artifacts.

Discussion

Our study demonstrated that thin-slice coronal TSE-DWI on 3T MRI yields a superior image quality and lesion conspicuity for assessment of hand lesions with acceptable image

noise. The scan time for TSE-DWI was 37% longer than that for EPI-DWI (196 and 143 s, respectively), with similar resolution. Nevertheless, in three cases including the case in Fig. 3, lesion conspicuity and overall image quality were rated as score 1 on EPI-DWI images and the lesion could not be evaluated at all in contrast to TSE-DWI. No cases were excluded due to motion artifacts despite the increase in scan time. In addition, MRI examination evaluating a hand lesion accounts for only 0.97% in our institution. So, the scan time might be considered acceptable. The thin-slice coronal DWI scan in our study can cover a larger area of the hand than axial DWI with a near-2-mm iso-voxel ($1.9 \times 1.9 \times 2.0 \text{ mm}$, slice gap: 0.2 mm) but was affected by severe distortion artifacts when using conventional EPI-DWI. TSE-DWI reduced these distortion artifacts, as reported in evaluations of various other lesions.^{1,5–10} However, severe image noise due to the characteristic of TSE-DWI and the necessity of a thinner slice might be problematic. To the best of our knowledge, this study represents the first use of TSE-DWI in evaluating lesions of the hand.

Diffusion-weighted imaging uses diffusion-sensitive echo preparations and reflects the random motion of water molecules in biological tissues. The greatest technical difficulty in DWI is to overcome the macroscopic tissue motion, while retaining sensitivity to microscopic water motion. A single-shot EPI sequence has therefore been most commonly used for DWI to acquire data more rapidly.^{1,4} However, severe image distortion, observed at the interfaces of

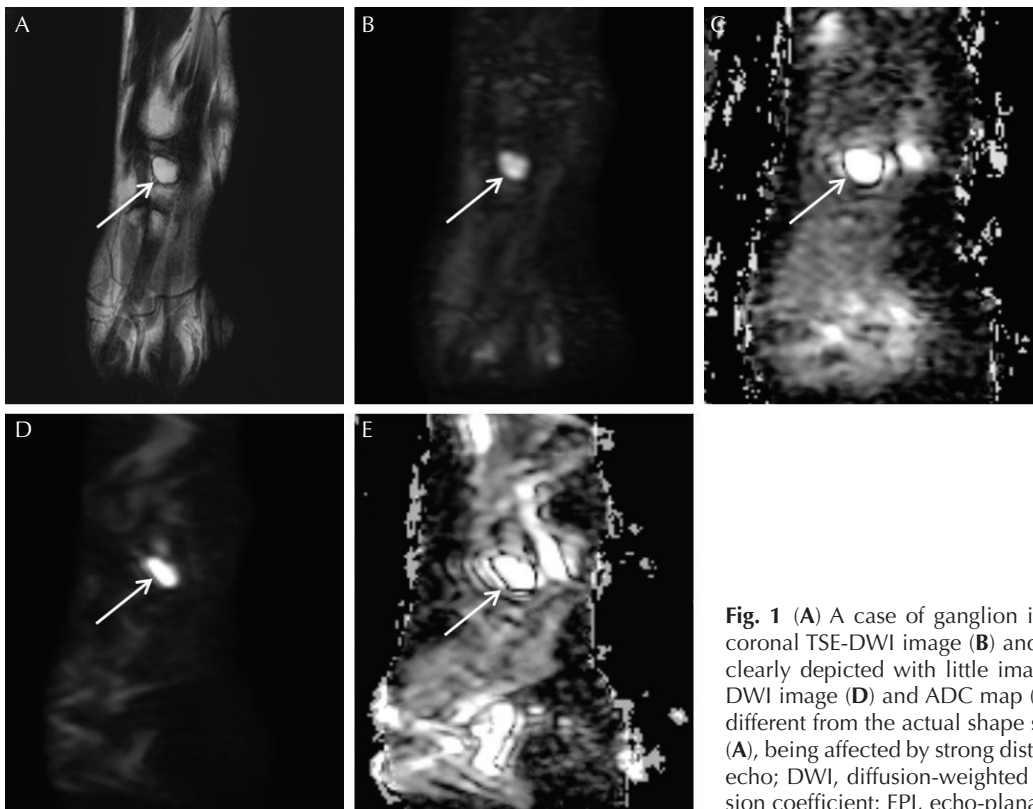


Fig. 1 (A) A case of ganglion in the right wrist joint. On the coronal TSE-DWI image (B) and ADC map (C), the lesion was clearly depicted with little image noise. On the coronal EPI-DWI image (D) and ADC map (E), the shape of the lesion was different from the actual shape shown on a T₂-weighted image (A), being affected by strong distortion artifacts. TSE, turbo spin-echo; DWI, diffusion-weighted imaging; ADC, apparent diffusion coefficient; EPI, echo-planar imaging.

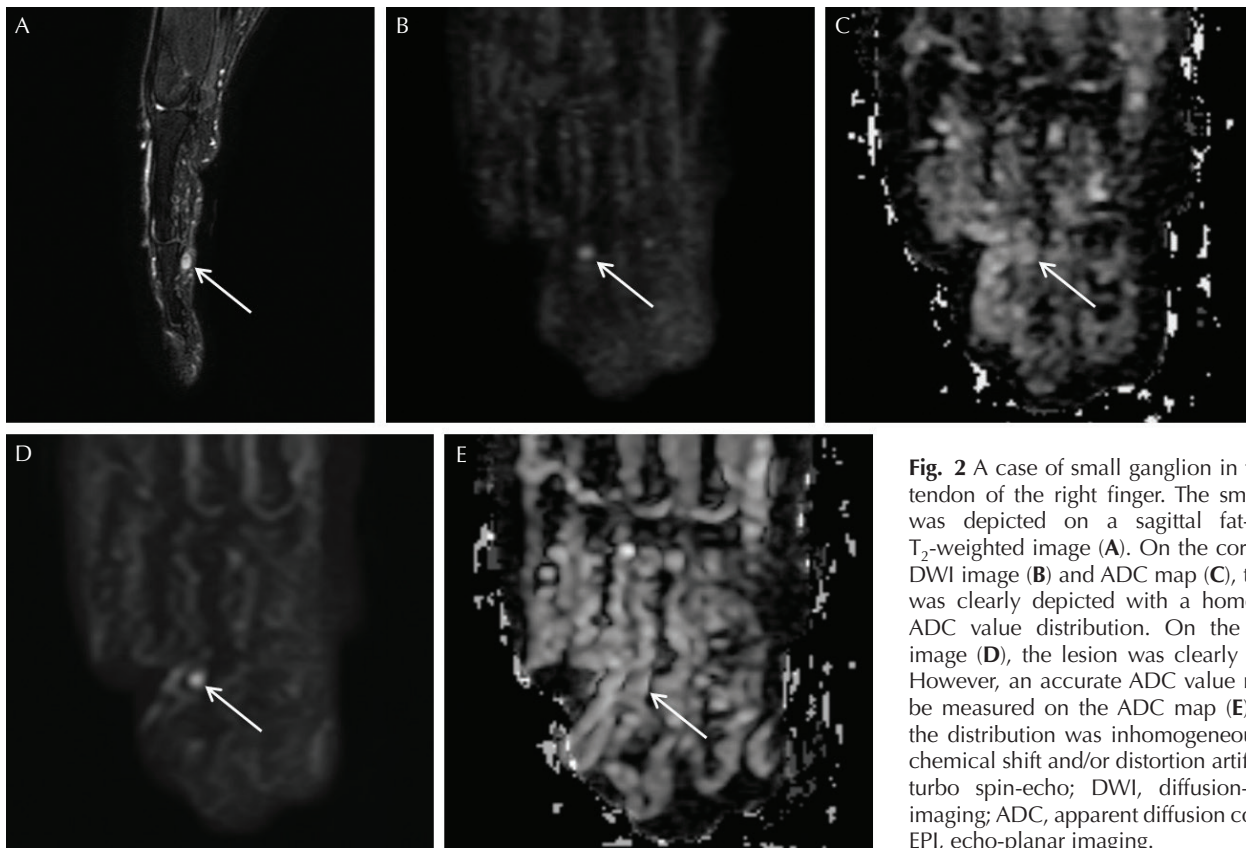


Fig. 2 A case of small ganglion in the flexor tendon of the right finger. The small lesion was depicted on a sagittal fat-saturated T₂-weighted image (A). On the coronal TSE-DWI image (B) and ADC map (C), the lesion was clearly depicted with a homogeneous ADC value distribution. On the EPI-DWI image (D), the lesion was clearly depicted. However, an accurate ADC value might not be measured on the ADC map (E) because the distribution was inhomogeneous due to chemical shift and/or distortion artifacts. TSE, turbo spin-echo; DWI, diffusion-weighted imaging; ADC, apparent diffusion coefficient; EPI, echo-planar imaging.

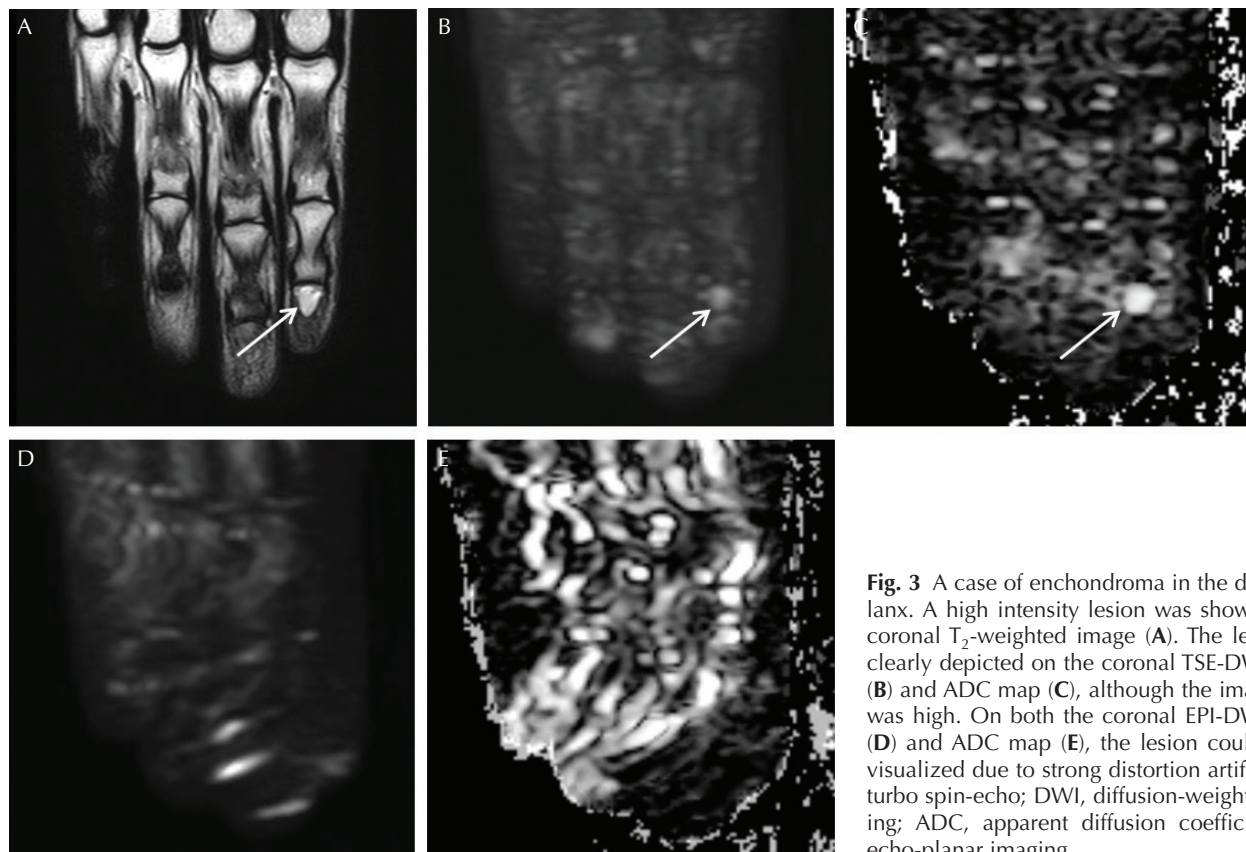


Fig. 3 A case of enchondroma in the distal phalanx. A high intensity lesion was shown on the coronal T₂-weighted image (A). The lesion was clearly depicted on the coronal TSE-DWI image (B) and ADC map (C), although the image noise was high. On both the coronal EPI-DWI image (D) and ADC map (E), the lesion could not be visualized due to strong distortion artifacts. TSE, turbo spin-echo; DWI, diffusion-weighted imaging; ADC, apparent diffusion coefficient; EPI, echo-planar imaging.

different susceptibilities, and chemical shift artifacts often cause image quality degeneration and inaccurate ADC measurements.^{1,4} In overcoming this issue, a post-processing software could be used to correct misregistration due to eddy-current-induced distortion for specific analyses in diffusion-tensor imaging but is not used for ADC measurement in daily practice. The multi-shot EPI sequence was demonstrated to reduce image distortion artifacts, but the strong susceptibility effect still caused image distortion, especially in non-brain imaging. In addition, increased image noise, scan times, and motion effects might remain problematic.¹ TSE-DWI was also developed to reduce image distortion and chemical shift artifacts. TSE-DWI uses a 180° radio-frequency refocusing pulse for each measured echo, which explains the strong reduction of the susceptibility artifacts.^{1,4,5,7-9} One of the problems with TSE-DWI has been motion artifacts resulting from the slower data acquisition. Nevertheless, combined use of the single-shot technique and parallel imaging technique, which is generally used for breath-hold ultrafast T₂-weighted imaging, was recently enabled for this TSE-DWI sequence. The single-shot technique with half-Fourier acquisition reduces motion artifacts. Single-shot TSE-DWI has issues with a low SNR and severe image blurring, but development of a multichannel coil and parallel imaging technique has increased the SNR and reduced shot duration, consequently reducing image blurring.⁴ In recent studies, TSE-DWI was found to be useful for visualizing chest lesions and enabled accurate ADC measurement of head and neck lesions due to fewer artifacts.^{7,8} Hiwatashi et al.¹ reported that TSE-DWI showed better diagnostic performance than multi-shot EPI-DWI when differentiating orbital lymphomas from inflammation. In our study of hand lesions, TSE-DWI showed higher scores for lesion conspicuity, image distortion, and overall image quality for both readers, with moderate to perfect inter-observer agreement. For the representative cases shown in Figs. 2 and 3, severe distortion artifacts prevented accurate ADC measurement or visualization of the lesion on EPI-DWI images, unlike TSE-DWI.

Clinically, the main problem of single-shot TSE-DWI with parallel imaging was the low SNR mentioned above. We used a 2-mm slice thickness, so the SNR was thought to be lower due to the thinner slice in our DWI study. Previous reports suggested that TSE-DWI yielded inferior lesion visibility compared with EPI-DWI because of the low SNR, although distortion artifacts on ADC maps of EPI-DWI had a negative effect on ADC measurements.^{5,10} Furthermore, precise ADC values cannot be obtained from DWI images with insufficient SNR because the errors in ADC value calculation are caused by strong image noise on the DWI images.² We calculated SNR of the DWI images but it is generally impossible to calculate a true SNR on clinical MRI images because the image noise in a single image is spatially inhomogeneous due to the use of parallel imaging, reconstruction filter, and susceptibility effect.¹¹ It is therefore preferable to investigate the concordance of ADC values in the

same lesions among different measurement methods or different examiners on multiple measurements. In our study, the image noise for TSE-DWI was objectively and visually higher than EPI-DWI. Nevertheless, there were no significant differences in visual score assessment for the two readers. In the ADC measurement assessment, ADC values for TSE-DWI and EPI-DWI showed excellent agreement (ICC = 0.97–0.99) with excellent inter-observer agreement (ICC = 0.98–1.00). Therefore, the SNR was thought to be sufficient for precise ADC value calculation without errors in our study. In addition, we used a 3T MRI scanner to increase the SNR compared to 1.5T MRI.⁸ The potential increase of distortion artifacts due to the higher magnetic field was solved by our use of the TSE technique.

Our study had several limitations. First, the ROIs in the tumors were manually placed. Small ROIs were placed on the artifact-free area showing visually lowest values on the ADC map for minimum ADC measurement according to previous studies.^{2,12} The larger ROIs placed in the whole lesion might include larger artifact areas for average ADC measurement. Nevertheless, excellent agreements of ADC values between TSE-DWI and EPI-DWI were obtained (ICC = 0.97–0.99) with excellent inter-observer agreement, and the reliability was confirmed for minimum and average ADC measurements. Second, the required sample size was calculated for visual score assessment, which was the primary endpoint of the study. We could not measure ADC values for lesions that were non-visible or suffered from artifacts on ADC maps, so fewer patients were included in our assessment of ADC measurement ($n = 15$). Nevertheless, agreements of the ADC values between TSE-DWI and EPI-DWI and between the observers were excellent. Third, malignant lesions were not included in this study. Malignant hand tumors are very few, so accumulating enough numbers of samples was difficult. Additionally, our purpose was to evaluate thin-slice TSE-DWI optimizing DWI technique for small hand lesions and detailed structures, and not to compare malignant tumors with benign tumors. Differentiation between malignant and benign musculoskeletal tumors was reported in many previous studies.² Fourth, we included the patients with no lesion or a postoperative change. We thought it is also important to diagnose the status as no lesion because DWI is often used for screening. However, we could not calculate the diagnostic accuracy and the influence of postoperative susceptibility effect was uncertain. It seems preferable to separately examine patients with a lesion, no lesion, and a postoperative change. Further studies with greater numbers of patients are warranted.

Conclusion

Thin-slice coronal TSE-DWI with recently developed techniques on 3T MRI was superior to conventional EPI-DWI in terms of less image distortion, allowing evaluation of a large area of the hand with near iso-voxel. Furthermore,

assessments of visual score and objective ADC measurement proved that the image noise, the major problem of thin-slice TSE-DWI, was acceptable.

Conflicts of Interest

The authors declare that they have no conflict of interest.

References

1. Hiwatashi A, Togao O, Yamashita K, et al. Diffusivity of intraorbital lymphoma vs. inflammation: comparison of single shot turbo spin echo and multishot echo planar imaging techniques. *Eur Radiol* 2018; 28:325–330.
2. Ogawa M, Kan H, Arai N, et al. Differentiation between malignant and benign musculoskeletal tumors using diffusion kurtosis imaging. *Skeletal Radiol* 2019; 48: 285–292.
3. Li X, Liu X, Du X, Ye Z. Diffusion-weighted MR imaging for assessing synovitis of wrist and hand in patients with rheumatoid arthritis: a feasibility study. *Magn Reson Imaging* 2014; 32:350–353.
4. Yoshida T, Urikura A, Shirata K, Nakaya Y, Terashima S, Hosokawa Y. Image quality assessment of single-shot turbo spin echo diffusion-weighted imaging with parallel imaging technique: a phantom study. *Br J Radiol* 2016; 89:20160512.
5. Baltzer PA, Renz DM, Herrmann KH, et al. Diffusion-weighted imaging (DWI) in MR mammography (MRM): clinical comparison of echo planar imaging (EPI) and half-Fourier single-shot turbo spin echo (HASTE) diffusion techniques. *Eur Radiol* 2009; 19:1612–1620.
6. De Foer B, Vercruyssen JP, Pilet B, et al. Single-shot, turbo spin-echo, diffusion-weighted imaging versus spin-echo-planar, diffusion-weighted imaging in the detection of acquired middle ear cholesteatoma. *AJNR Am J Neuroradiol* 2006; 27:1480–1482.
7. de Graaf P, Pouwels PJ, Rodjan F, et al. Single-shot turbo spin-echo diffusion-weighted imaging for retinoblastoma: initial experience. *AJNR Am J Neuroradiol* 2012; 33: 110–118.
8. Ohno Y, Koyama H, Yoshikawa T, et al. Diffusion-weighted MR imaging using FASE sequence for 3T MR system: preliminary comparison of capability for N-stage assessment by means of diffusion-weighted MR imaging using EPI sequence, STIR FASE imaging and FDG PET/CT for non-small cell lung cancer patients. *Eur J Radiol* 2015; 84:2321–2331.
9. Özgen B, Bulut E, Dolgun A, Bajin MD, Sennaroğlu L. Accuracy of turbo spin-echo diffusion-weighted imaging signal intensity measurements for the diagnosis of cholesteatoma. *Diagn Interv Radiol* 2017; 23:300–306.
10. Verhappen MH, Pouwels PJ, Ljumanovic R, et al. Diffusion-weighted MR imaging in head and neck cancer: comparison between half-fourier acquired single-shot turbo spin-echo and EPI techniques. *AJNR Am J Neuroradiol* 2012; 33:1239–1246.
11. Ogawa M, Kawai T, Kan H, et al. Shortened breath-hold contrast-enhanced MRI of the liver using a new parallel imaging technique, CAIPIRINHA (controlled aliasing in parallel imaging results in higher acceleration): a comparison with conventional GRAPPA technique. *Abdom Imaging* 2015; 40:3091–3098.
12. Oka K, Yakushiji T, Sato H, Hirai T, Yamashita Y, Mizuta H. The value of diffusion-weighted imaging for monitoring the chemotherapeutic response of osteosarcoma: a comparison between average apparent diffusion coefficient and minimum apparent diffusion coefficient. *Skeletal Radiol* 2010; 39:141–146.